RESEARCH PAPER

Green Synthesis of Titanium oxide nanoparticles using *Eucalyptus* leaves; Characterisation and its Potential in Methylene Blue Pollutant degradation with light

Suresh K C[1]

[1]*Department of Physics, Government First Grade Women's College, Tumkur-572102, Karnataka, India*

Corresponding author email: kunigalsuresh@gmail.com

Abstract

In this study, titanium oxide (TiO_2) nanoparticles were fabricated from a green route using fresh and healthy *eucalyptus leaf* extract. The structural and morphological evaluation was done using X-ray diffraction (XRD), scanning electron microscopy (SEM), high-resolution transmission electron microscopy (HRTEM), selected area electron diffraction (SAED), energy-dispersive X-ray spectroscopy (EDX), BET specific surface area and porosity. The optical properties were explored from photoluminescence (PL), and UV–Vis spectroscopy. The blended TiO_2 nanoparticles revealed an average crystalline size range of 84.65 nm with a comparatively higher specific surface area. SEM and HRTEM profiles explored the spherical and faceted structure which is clumped together in an agglomerated form. The broader green emission band was shown in PL study, typically centered around 506–544 nm, is substantiated anatase phase of TiO_2 nanoparticles. Thermal stability was assessed through TGA and found prepared TiO_2 nanoparticles were immensely stable beyond 385 °C. The U-V absorption peak found at 344 nm and optical band gaps; 2.82 eV and 3.01 eV was ascertained using the Tauc plot and the photocatalytic performance of the TiO_2 nanoparticle as a photocatalyst for methylene blue dye under UV light irradiation was explored and it exhibited 95.48 % degradation in 140 min.

Key words: TiO_2 nanoparticles; Green synthesis; structural analysis; XRD; SEM; HRTEM; BET; Photocatalytic activity;

How to cite this article: SureK C. Green Synthesis of Titanium oxide nanoparticles using Eucalyptus leaves; Characterisation and its Potential in Methylene Blue Pollutant degradation with light. Int J Drug Deliv Technol. 2026;16(79s):584-592. DOI: 10.25258/ijddt.16.79s.111.

1. Introduction

Advances in industrial and agricultural domain have often led to increased pollution, especially in aquatic areas. The health of living things and the environment's ecosystem as a whole negatively impacted by aquatic pollutants. As a result, several nations focused their efforts on determining the lowest levels of these pollutants at which they were legally required. However, safeguarding water sources and developing innovative water treatment technologies have grown to resolve the environmental issues in the twenty-first century [1]. Numerous methods, adsorption, oxidation, photocatalysis, and microbial decomposition was employed to treat effluent. Because of the affordability and ease of use, photocatalysis has drawn the most interest among these techniques [2]. Researchers are particularly interested in creating efficient catalytic materials that activate when exposed to visible light. [3].

Global population rate has greatly influenced the demand for textile products, which increases the use of synthetic dyes. This increases the usage of wastewater from dye industries, textile manufacturing, leather making, and paper printing. Furthermore, the majority of organic dyes, detergents, and pesticides contain toxic substances, which cannot be removed easily from the environment. Hence, a sophisticated, extremely effective and environmentally friendly route for treating dye pollution, metal oxide nanoparticle photocatalyst based dye degradation to convert complex, hazardous organic colors from texti le effluents into harmless byproducts like carbon dioxide and water. Green blended TiO_2 nanoparticles can be used as a photocatalyst, as it is found to be stable, economical, high Uv light absorption capacity and safe for the environment [4,5]. There are several methods to fabricate different metal oxide nanoparticles for diverse applications. According to research reports, titanium dioxide nanoparticles could be synthesized through chemical and biological methods. Chemical routes viz, sol-gel method [6], solvo-thermal method [7], co-precipitation method [8], hydrothermal method [9], uses toxic chemicals as well as the synthesis involves high temperature and pressure which leads to limitations in mass production of TiO_2 nanoparticles. Hence, bio-synthesis of nanomaterials is getting increased attention because easy, ecofriendly, and nontoxic to nature, and it involves the use of biological sources as reducing agents which are derived from plants and their wastes, fruit extract and microorganisms are utilized in the synthesis [10-12]. Especially, plant extracts serve as effective reducing and capping agents for nanoparticles synthesis, offering benefits over microbial methods by eliminating the complex procedures of cell culturing and maintenance. Plants can accumulate heavy metals in leaves, roots, fruits, etc. Therefore, synthesis using plant extracts attract attention as simple, effective, cheap and feasible methods for obtaining nanoparticles. Metal oxide nanoparticles by green synthesis are very productive for obtaining monodisperse nanoparticles with desired morphologies [13]. Pure metallic nanoparticles of gold and silver are synthesized for direct usage, from plant leaf extracts and [14,15]. Different metal oxides like, nickel oxide [16], Tin oxide [17], zinc oxide [18], copper oxide [19], silver oxide [20], gold oxides nanoparticles [21] have broad applications environmental section. Among these metal oxide nanoparticles, tin oxide stands out as a notable biocompatible option, as it is, safe cost-effective, and possesses a high refractive index along with an excellent UV-absorbing quality [22]. Also, they have a wide range of applications, such as, reducing the adverse effects of dyes used in the textile industry by photodegradation of pollutant water treatment, energy storage, gas sensing, food industries, etc., Therefore, green blended tin oxide nanoparticles are gaining recognition in agricultural, environmental, and industrial fields [23].

In lieu of the above discussion, Herein, the current report focuses on the potential study of green synthesis of titanium TiO_2 nanoparticles using *eucalyptus* leaves, morphological and structural characteristics of nanoparticles from UV-Vis, XRD, SEM, HRTEM, EDX, SAED, FTIR, BET and photoluminescence. Further, these nanoparticles were used to scrutinize photodegradation of methylene blue dye.

2. Materials and Procedures

2.1 Preparation of eucalyptus extract

Fresh, healthy eucalyptus leaves were collected from a village in Karnataka, Tumkur district, India. Then, the compiled leaves were carefully cleansed with deionized water (DI) to eliminate any dirt and moisture. After being washed, the leaves were collected and dried for ten to twelve days at room temperature. Dried leaves are finely powdered using a home mixer (mixie). 10 g of the powdered leaf was added to 300 mL of distilled water in a 500 mL conical flask. The mixture was then boiled for 60 minutes at an elevated temperature of 80°C using a magnetic stirrer on a hot plate, and it was cooled to room temperature. The solution was filtered using Whatman No. 1 filter paper to remove the remnants and get a clear aqueous extract of eucalyptus leaves. This filtrate was stored in the refrigerator for further use.

2.2 Synthesis of TiO_2 nanostructures

The base solution was prepared by adding 50 mL of 0.2 M, Titanium isopropoxide (Merck grade, India) precursor to 200 mL of *eucalyptus* leaf extract and stirred using a magnetic starrier on hot plate for 6 hours at elevated temperature of 80°C. The mixture is cooled down to room temperature and the precipitate is filtered and being washed multiple using absolute ethanol by centrifuging at 10,000 rpm. The precipitate was dried in hot air oven at 80°C, overnight and then it is calcinated at 400°C for 60 minutes. The resultant product was termed as TiO_2 nanoparticles. The technique for production, characterization, and application of TiO_2 nanoparticles is shown below.

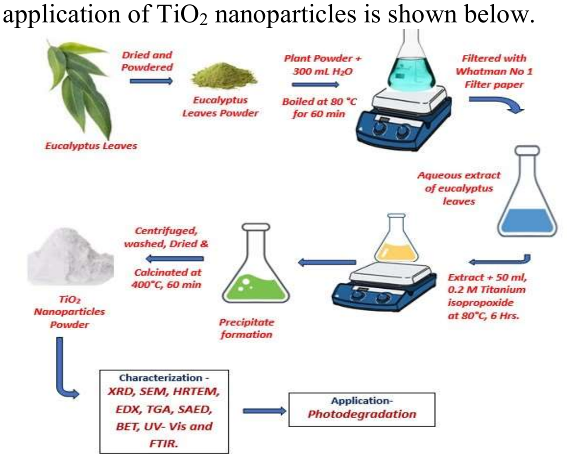

Protocol of Production, characterization of TiO_2 nanoparticles

2.3 Sample preparation for photocatalytic activity

The 5 mg of prepared TiO_2 nanoparticles photocatalyst settled in a 100 mL aqueous solution of methylene blue (2 g/L) dye at neutral pH. The dye solution containing TiO_2 nanoparticles is continuously stirred using a magnetic stirrer to reach a state of adsorption-desorption equilibrium. Once this equilibrium is achieved, the solution is placed in a UV chamber for further processing. Subsequently, UV-visible absorption spectra were measured to examine the adsorption performance of MB dye before (0 min) and after every 20 min of irradiation. All the UV-vis absorption spectral measurement was done at room temperature. The MB dye degradation performance was studied with and without TiO_2 photocatalyst in presence and absence of light using UV chamber.

The photocatalytic dye degradation efficiency of the blended TiO_2 nanoparticles was computed by using the following equation (1)

$$\eta = \left(\frac{C_o - C_t}{C_o}\right) 100 \quad \text{------(1)}$$

Here, η is the degradation percentage, C_o the initial absorbance of dye at 00 min, C_t is the change in absorbance at regular intervals of 20 min of the degradation [16].

3 Characterization techniques

The morphology and crystalline nature of the synthesized samples were evaluated by an X-ray diffractometer PANalytical X'Pert Pro MPD equipped with a Cu K_α (λ = 1.5418 Å) as a radiation source [16].

The green blended samples were analyzed over the 2θ range from 20 to 80° at room temperature. The high-resolution transmission electron microscopy (HRTEM) images were obtained using a JEOL JEM 2100 Plus (Germany). A high-resolution FESEM image was recorded using TESCAN MIRA.

The Fourier transforms infrared (FTIR) spectra of the TiO_2 nanoparticles were recorded using an FTIR spectrophotometer Bruker, USA. The spectra were recorded in the range between 4000 and 500 cm^{-1}. The optical absorption spectra and photocatalytic activity of the fabricated TiO_2 nanoparticles were conducted by UV-visible spectrophotometer (Shimadzu; Japan) and the nanostructure spectra was recorded 200-1400 nm. The specific surface area (SBET) was calculated using the Brunauer–Emmett–Teller (BET) process using a BET surface area analyzer (Microtrac – BELSORP MINI X). The sample was processed for three hours at 350 K in a vacuum to eliminate physisorbed moisture or any adsorbed gases from the surface of the material without affecting the sample structure.

4. Results and discussions

4.1 XRD study of TiO_2 nanoparticles

The TiO_2 nanoparticles' XRD patterns were shown in Fig. 1. TiO_2 nanoparticles' highly crystalline tetragonal structure was validated by XRD evaluations. The diffracted angle values obtained from XRD pattern for TiO_2 nanoparticles are 27.44°,36.08°,39.03°,41.25°, 44.05°,54.32°,56.63°, 62.76°, 64.04°, 69.00°, 69.79° and 76.54°. XRD pattern confirmed high-quality anatase crystalline structure. Sharp and intense peaks were observed The XRD patterns results reveals that the structure of TiO_2 was mixed phase of anatase with and rutile. The XRD pattern's diffracted angles accord well with the conventional JCPDS file No. 21-1272 (anatase phase) and JCPDS file No. 21-1276 (rutile phase) [25].

The following Debye Scherer Eq. (2) used to determine the crystallite size [26].

$$D = \frac{k\lambda}{\beta cos\theta} \quad \text{------ (2)}$$

Here K is constant 0.98, λ is x-ray wavelength, θ is the angle of diffraction, β is full width half maxima. The average crystallite size of the green-synthesized TiO2 nanoparticles was 85.64 nm.

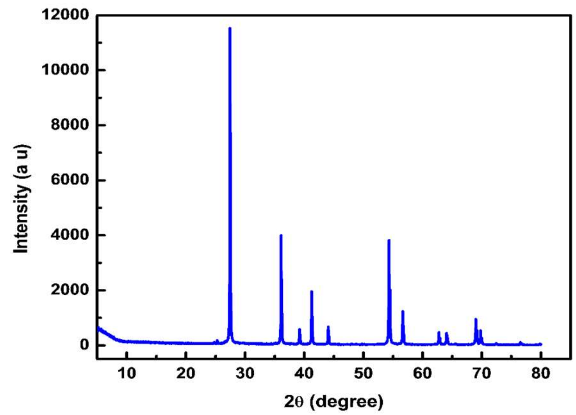

Fig. 1 XRD pattern for TiO_2 nanoparticles

4.2 Morphological studies of TiO_2 nanoparticles

The green derived TiO_2 nanoparticles' SEM micro and nanostructure images are displayed in Figs. (a, b, and c). It demonstrates the irregularity of the produced TiO2 particles, some of which have spherical and faceted structures and are clustered together in an agglomerated contour. The SEM also depicts quasi-spherical aggregated surface morphology.

The compositional analyses of the prepared sample with the presented elements by EDX spectrum are illustrated in Fig 2 (d). The elements encapsulated in the blended nanoparticles have

Fig 2 SEM images (a, b & c) of EDX pattern (d) of TiO_2 nanoparticles

been recorded by an EDX spectrum, which further verifies the presence of Ti with 54.57 % and O with 41.54% with fraction of copper (1.66 %) and mentioned table 1

Table 1

Element	Atom %	Weight %
Ti K	69.52	54.57
O K	28.84	41.54
Cu K	01.66	03.89
Total	100	100

Fig. 3 TEM and HRTEM characterization TiO_2 nanoparticles (a-h) SAED Pattern (i)

The morphology of TiO_2 nanostructure was characterized by TEM and HRTEM, as depicted in Fig 3 (a-h). TEM micrograph illustrate TiO_2 is a mixture of anatase and rutile phase. Cuboidal shaped particle morphology with a size about 339.4 nm in length, 187.3 nm in width with the thickness 120.72 nm. Some irregularly shaped particles were seen in the TEM micrograph. Particles agglomerated in rhombic profile facet were rendered in the image.

4.3 Optical Properties

UV–visible absorption spectra were recorded to perceive the optical properties of synthesized TiO_2

nanoparticles. The Fig 4(a) represented the UV–vis absorption spectra of depicted that UV absorption peaks at 344 nm, which shows the existence of TiO_2 nanoparticles as reported by elsewhere [26] in the earlier studies. From the absorption spectra, the indirect and direct band gap energy values of TiO_2 nanoparticles were obtained using standard Tauc relation.

$$\alpha(\nu)h\nu = K\left(h\nu - E_g\right)^n$$

α(ν) is absorption coefficient, K is a constant, E_g is energy bandgap, hν is incident photon energy, and n equals to ½ for direct bandgap semiconductor and equals to 2 for indirect band gap semiconductors.

Fig.4 UV–vis absorption spectra and Tauc plot of

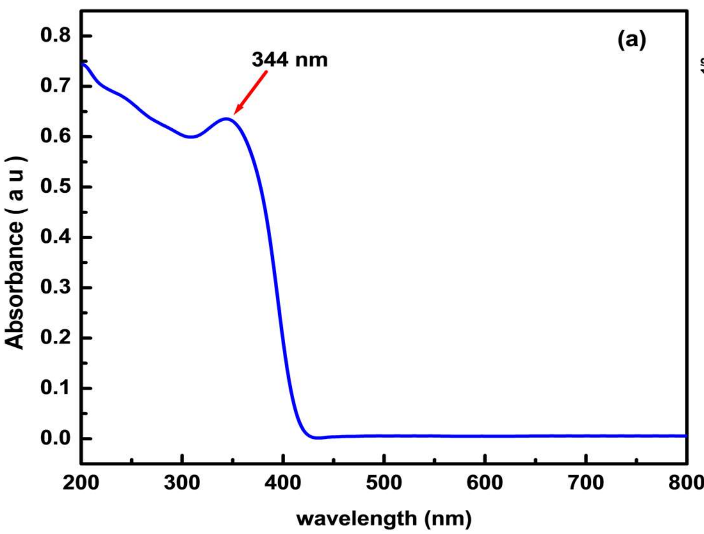

prepared TiO_2 nanoparticles

A Tauc plot of the indirect band gap [$(\alpha\ h\nu)^{1/2}$ vs hν] and direct band gap [$(\alpha h\nu)^2$ vs hν] respectively is presented in the Fig. 4(b) and 2(c). The indirect band gap was calculated and found to be 2.82 eV. On the other hand, green produced TiO_2 nanoparticles had direct band gap value of 3.01 eV. These values are close agreement with the earlier report [29].

4.4 FTIR evaluation

FTIR spectra of TiO_2 nanoparticles is exhibited in Fig.5 and prominent peaks are observed at 3332, 1645, 1138, and 505 cm^{-1}. The strong and broad absorbance bands at 3332 cm^{-1} are known to be associated with the stretching O–H stretching and adsorbed water molecules on the nanoparticles surface. The existence of these groups was common in green synthesis of nanomaterials. The band corresponds to 1645 cm^{-1} depicts bending vibration of adsorbed molecular water and O-H bending. The band observed at 1138 cm^{-1} is because of C–O stretching vibrations indicates organic residues, from the plant extract used for synthesis, which act as capping or stabilizing agents. A band at 505 cm^{-1} in FTIR suggested O–Ti–O bonding reported elsewhere [29-31]. These absorption peaks demonstrate the existence of surface moisture and organic functional groups the fundamental Ti-O bonding, which is the typical characteristic of formation of TiO_2 nanoparticles, further confirm the role of the biogenic material as a stabilizing and capping agent during the green synthesis.

.

Fig. 5 FTIR Spectra of green synthesised TiO_2 nanoparticles in the range 500-4000 cm^{-1}

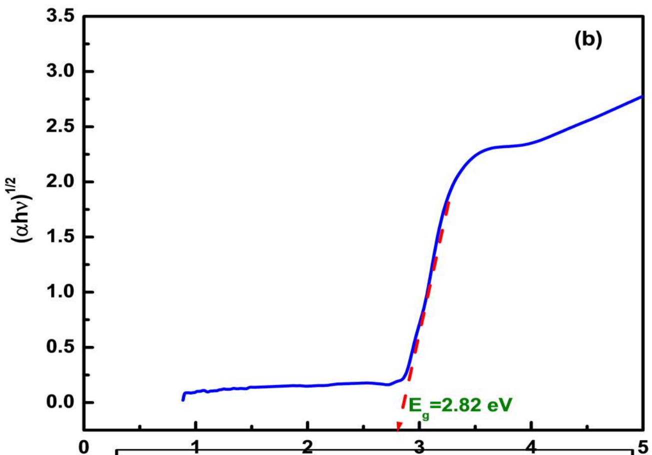

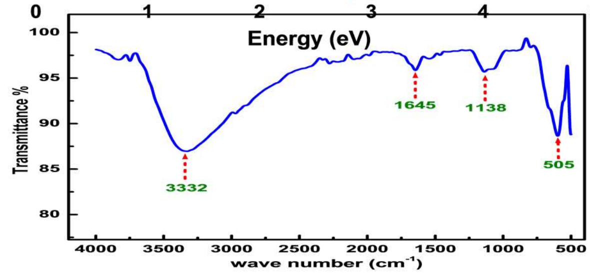

4.5 Specific surface area analysis

The photocatalytic activity of TiO_2 nanoparticles relies on their surface area and bandgap energy. TiO_2 nanoparticles with a larger surface area have excellent photocatalytic activity. Hence the active surface area of the TiO_2 nanoparticles was measured. The N_2 adsorption–desorption isotherm of green prepared TiO_2 nanoparticles is presented in Fig. 6(a). The observed Brunauer–Emmett–Teller (BET) surface area, pore size, and pore volume of TiO_2 nanoparticles are mentioned in Table 2 from BET Plot.

The amount of N_2 adsorption rapidly increases beyond the relative pressure of 0.5 and hence, adsorption and desorption profile show a hysteresis loop at higher relative pressure, reflected the porous essence of the compound.

Table 2

Sample	BET Surface area(m^2g^{-1})	Pore diameter (nm)	Pore volume(ccg^{-1})
TiO_2	15.55	9.46	0.07354

Barrett-Joyner-Halenda (BJH) method to analyze their pore size distribution and these properties are crucial as they significantly influence the nanoparticles performance in applications such as photocatalysis and adsorption. The BJH plot for green synthesized TiO_2 nanoparticles is shown in the Fig. 6(b). It indicates that the nanoparticles contain high concentration very small pores from 1 - 10 nm and decreasing concentration of pores larger than 10 nm.

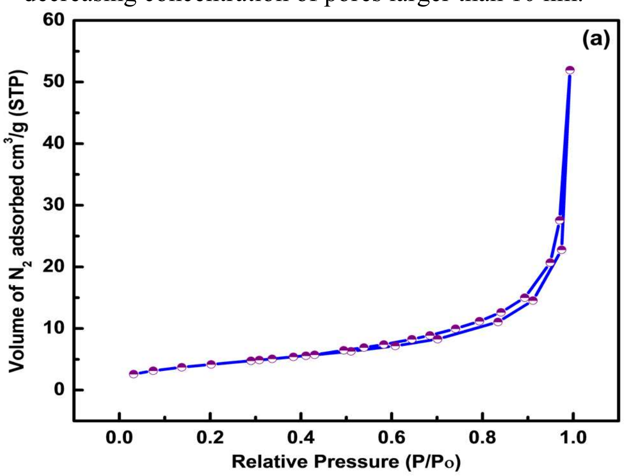

Fig. 6 Adsorption-desorption isotherm (a) and BJH pore size distribution curve (b)
green synthesised TiO_2 nanoparticles with relative pressure 0-0.1 range

4.6 Photoluminescence

The photoluminescence (PL) excitation and emission spectrum of TiO_2 nanoparticles at room temperature is illustrated in Fig. 7. The phytochemicals in the plant extract impact the crystallization process. The organic molecules from the plant extract act as a reducing agent during synthesis and can be adsorbed onto the TiO_2 nanoparticle surface. These organic capping agents and phytochemicals can also create defect states or alter the surface electron structure, leading to distinct emission peaks due to recombination of the photo generated charge carriers. The PL emission spectrum was recorded using excitation wavelength of 256 nm. The PL emission spectrum revealed the peaks at 434, 458, 506, 520 and 544 nm in TiO_2 nanoparticles.

The PL emission peaks at 434 and 458 nm attributed to recombination of trapped electrons in the oxygen vacancies with holes in the valence band. This emission is specifically due to surface and intrinsic defect states. The broader green emission band, typically centered around 506–544 nm, is a well-documented characteristic of anatase TiO_2 nanoparticles and is highly sensitive to surface properties and synthesis conditions [32]. This emission is primarily caused by oxygen vacancies formed below the conduction band and act as electron-trapping sites. This radiative recombination of an electron from an oxygen vacancy level with a hole in the valence band produces visible light. The presence of hydroxyl groupson the nanoparticle surface can also create additional surface defects and trapping states, contributing to the green luminescence. The organic

Fig. 7 Photoluminescence excitation (a) and emission (b) spectra of green synthesizedTiO_2 nanoparticles in the range 200-600 nm

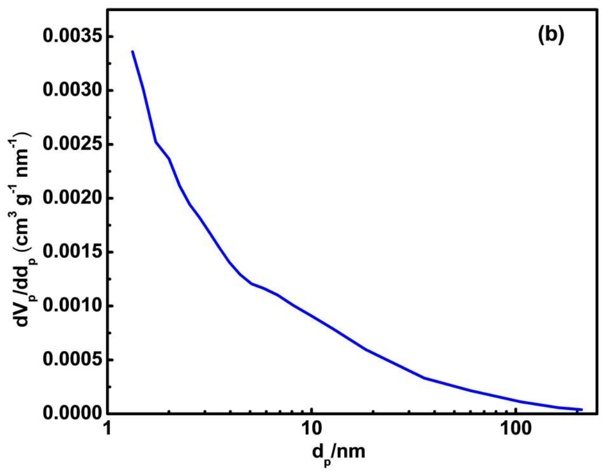

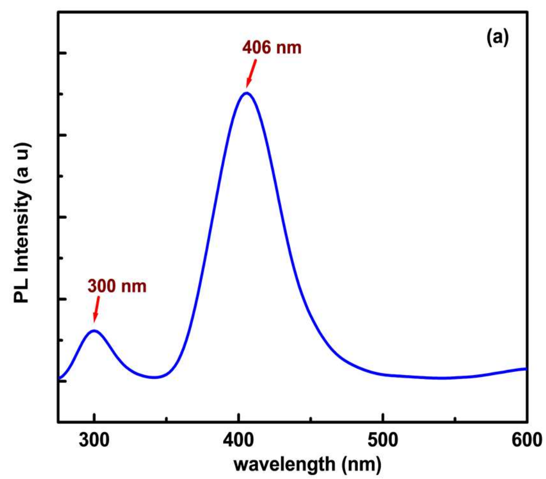

molecules from the plant extract act as a reducing agent during synthesis and can be adsorbed onto the TiO_2 nanoparticle surface. These organic capping agents and phytochemicals can also create defect states or alter the surface electron structure, leading to distinct emission peaks.

4.7 Thermal study of TiO_2 nanoparticles

The thermal gravimetric analysis (TGA) is carried out at a heating rate of 10 °C /min under nitrogen atmosphere over a temperature range from 25 °C to 900 °C. TGA profile curves of the blended TiO_2 nanoparticles are illustrated in Fig. 8. Two weight losses can be examined in the TGA curve.

Minor weight loss of 3.28 % was found up to the temperature 304 °C. This loss was due to the presence of water molecules of the lattice. It revealed that the TGA curve exhibit a weight loss of a sample as 24.90 % occurred in the temperature range from 304 to 385 °C as a consequence of the water evaporation and the organic components found in the eucalyptus leaf extract. Similar observation of weight loss of TiO_2 nanostructures is already reported [33].

Fig. 8 Thermogravimetric analysis of green synthesized TiO_2 nanoparticles

4.8 Photocatalytic activity

The global population rate increases the demand for textile products, leather products and paper printing. Methylene blue (MB) dye is said to be a common dye in the wastewater produced by textile factories, among other contaminants. These dyes and pollutants are carcinogenic, toxic and nonbiodegradable under natural atmospheric conditions. Hence, it has negative impact on the health of living organisms and the general condition of the environment. In this work, we have studied the photocatalytic capabilities of green fabricated TiO_2 nanoparticles against MB dye in UV chamber. The absorption Vs wavelength plotted and the absorption characteristic peak obtained at 663 nm. The effect of photocatalysis was determined by monitoring characteristics peak intensities. During the photocatalysis process, the decrease in the intensity of the absorption peak suggested a reduction in dye concentration, as demonstrated in the Fig 9 (a).

The MB dye degradation was also examined by plotting $\frac{C}{C_o}$with time in Fig. 9 (b). The relative concentration ratio was outlined the amount of MB dye degradation over time. The ratio $\frac{C}{C_o}$ almost stand to be constant with infinitesimal decrease in dye degradation in absence of light without TiO_2 nanoparticles photocatalyst, as there is no formation of active species to initiate photodegradation. Even in presence of photocatalyst, with the absence of light, there is very negligible decrease in the concentration ratio $\frac{C}{C_o}$ was observed and depicted in the Fig. 9 (b) with time first 20 min, because the active radicals could not be produced in the solution, which is needed for dye to degrade. However, a substantial and continuous decline in $\frac{C}{C_o}$ was observed, when the MB dye solution was suitably blended TiO_2 nanoparticles under light irradiation. This confirms the production of reactive oxygen species was produced and it was very much required for the degrade the dye. The decrease in the concentration ratio $\frac{C}{C_o}$ reaching nearly zero within 140 min shows enhanced performance of TiO_2 nanoparticles as photocatalyst.

Fig 9 (c) presented the photocatalytic degradation of MB dye over time under light irradiation in presence and absence of TiO_2 nanocomposites. In the absence of TiO_2 nanoparticles, MB dye degradation efficiency was minimum and remains constant over time, indicating that reaction species cannot form in dye solution and hence there is no noticeable degradation of dye. The presence of TiO_2 photocatalyst in the dye solution generates active species when exposed to light, leading to an extremely notable degradation efficiency of 87.63% with formation of carbon dioxide and water after 140 minutes of irradiation. This degradation of MB dye occurs through oxidation and decomposition processes, facilitated by TiO_2 nanoparticles which act as a photocatalyst. When a photon of light of significant wavelength is illuminated on the TiO_2 nanoparticles, excite electrons (e^-) from the valence band to the conduction band and leaves behind holes (h^+) in the valence band.

$$TiO_2 + h\nu -> e^- + h^+$$

These excitons produce high oxidizing power species of hydroxide radicals and superoxide anions. Demethylation mediated by these hydroxyl radicals and hydroxyl ions was found to be crucial process among the pathways analyzed, resulting in the generation of intermediates such as Azure B, methanol, and formaldehyde. The viability of demethylation as the first degrading step, which was demonstrated by the energetics of these reactions [34, 35].

They have strong capability to degrade methylene blue dye pollutant of waste water along with various other industrial waste effluents from the reactions between the generated excitons and oxygen or water. Pollutant MB dye was entirely broken down into carbon dioxide, water, ammonium ions and sulfate groups and inorganic compounds and the mechanism as shown in Fig.9(d).

$$e^- + O_2 -> \cdot O_2^-$$

$$h^+ + H_2O -> OH^{\cdot} + H^+$$

$$MB\ Dye + \cdot O_2^- + OH^{\cdot} - > H_2O + CO_2 + NH^{4+} + SO_4^{2-}$$

The absorption Vs wavelength plot depicting the decrement in absorbance of MB using TiO_2 photocatalyst portrayed 87.63 % degradation in 140 min and had been reported in previous work [36,37].

Fig. 9 Photocatalytic degradation responses and mechanism of
TiO_2 nanoparticles on MB dye (a, b, c & d)

5. Conclusions

Using *eucalyptus* leaf extract, titanium dioxide nanoparticles were successfully manufactured using green technologies. The phytochemicals in the e*ucalyptus* leaf extract successfully acted as both reducing and stabilizing agents to form TiO_2 nanoparticles. The fabricated TiO_2 nanoparticles were rigorously investigated through XRD, SEM, HRTEM, EDX, SAED, TGA, BET, PL, UV- Vis and FTIR. The blended TiO_2 nanoparticles revealed an average crystalline size range of 84.65 nm with specific surface area of 71.89 m^2g^{-1}. SEM and HETEM study explored the spherical and faceted structure which is clumped together in an agglomerated form.PL emission spectra between 506–544 nm validated anatase phase of TiO_2 nanoparticles. TGA profile shows TiO_2 nanoparticles were immensely stable and exhibit photodegradation of 95.48 % in 140 min on UV light irradiation. Hence, it is a feasible alternative for the degradation of contaminants from industrial wastes.

Declarations

Availability of data and materials: The data that support the findings of this study are available from the corresponding author K C Suresh, and shall be shared on reasonable request.

Competing interest: The author declare that they have no known competing financial interests or personal relationships that could have appeared to influence the work reported in this paper.

Funding: This research received no specific grant from any funding agency in the public, commercial, or not-for-profit sectors.

Authors Contributions: The author confirms sole responsibility for the study conception and design, data collection, analysis and interpretation of results, manuscript preparation and review.

Acknowledgement: The author thanks the editors for their assistance during the review process.

6. References

1) Mohammed, B. B., Yamni, K., Tijani, N., Alrashdi, A. A., Zouihri, H., Dehmani, Y., Chung, I., Kim, S., &Lgaz, H. (2019b). Adsorptive removal of phenol using faujasite-type Y zeolite: Adsorption isotherms, kinetics and grand canonical Monte Carlo simulation studies. *Journal of Molecular Liquids*, *296*, 111997. https://doi.org/10.1016/j.molliq.2019.111997.

2) Zinatloo-Ajabshir, S., Baladi, M., & Salavati-Niasari, M. (2020). Enhanced visible-light-driven photocatalytic performance for degradation of organic contaminants using PbWO4 nanostructure fabricated by a new, simple and green sonochemical approach. *Ultrasonics Sonochemistry*, *72*, 105420. https://doi.org/10.1016/j.ultsonch.2020.105420.

3) Mafa, P. J., Ntsendwana, B., Mamba, B. B., &Kuvarega, A. T. (2019). Visible light driven ZNMOO4/BIFEWO6/RGO Z-Scheme photocatalyst for the degradation of anthraquinonicdye.*The Journal of Physical Chemistry C*, *123*(33), 20605–20616. https://doi.org/10.1021/acs.jpcc.9b05008.

4) Elbadawy, H. A., Elhusseiny, A. F., Hussein, S. M., & Sadik, W. A. (2023). Sustainable and energy-efficient photocatalytic degradation of textile dye assisted by ecofriendly synthesized silver nanoparticles. *Scientific Reports*, *13*(1), 2302. https://doi.org/10.1038/s41598-023-29507-x

5) Shimi, A. K., Ahmed, H. M., Wahab, M., Katheria, S., Wabaidur, S. M., Eldesoky, G. E., Islam, M. A., & Rane, K. P. (2022). Synthesis and applications of green synthesized TIO2 nanoparticles for photocatalytic dye degradation and antibacterial activity. *Journal of Nanomaterials*, *2022*(1). https://doi.org/10.1155/2022/7060388

6) Sharma, R., Sarkar, A., Jha, R., Sharma, A. K., & Sharma, D. (2019). Sol-gel–mediated synthesis of TiO_2 nanocrystals: Structural, optical, and electrochemical properties. *International Journal of Applied Ceramic Technology*, *17*(3), 1400–1409. https://doi.org/10.1111/ijac.13439.

7) Ramakrishnan, V. M., Natarajan, M., Santhanam, A., Asokan, V., & Velauthapillai, D. (2017). Size controlled synthesis of TiO_2 nanoparticles by modified solvothermal method towards effective photo catalytic and photovoltaic applications. *Materials Research Bulletin*, *97*, 351–360. https://doi.org/10.1016/j.materresbull.2017.09.017.

8) Horti, N., Kamatagi, M., Patil, N., Nataraj, S., Sannaikar, & Inamdar, S. (2019). Synthesis and photoluminescence properties of titanium oxide (TiO_2) nanoparticles: Effect of calcination temperature. *Optik*, *194*, 163070. https://doi.org/10.1016/j.ijleo.2019.163070.

9) Wang, Z., Haidry, A. A., Xie, L., Zavabeti, A., Li, Z., Yin, W., Fomekong, R. L., & Saruhan, B. (2020). Acetone sensing applications of Ag modified TiO_2 porous nanoparticles synthesized via facile hydrothermal method. *Applied Surface Science*, *533*, 147383. https://doi.org/10.1016/j.apsusc.2020.147383.

10) Singh, J., Kumar, S., Alok, A., Upadhyay, S. K., Rawat, M., Tsang, D. C., Bolan, N., & Kim, K. (2019). The potential of green synthesized zinc oxide nanoparticles as nutrient source for plant growth. *Journal of Cleaner Production*, *214*, 1061–1070. https://doi.org/10.1016/j.jclepro.2019.01.018.

11) Rathi, V. H., & Jeice, A. R. (2023). Green fabrication of titanium dioxide nanoparticles and their applications in photocatalytic dye degradation and microbial activities. *Chemical Physics Impact*, *6*, 100197. https://doi.org/10.1016/j.chphi.2023.100197 .
12) Nadeem, M., Tungmunnithum, D., Hano, C., Abbasi, B. H., Hashmi, S. S., Ahmad, W., & Zahir, A. (2018). The current trends in the green syntheses of titanium oxide nanoparticles and their applications. *Green Chemistry Letters and Reviews*, *11*(4), 492–502. https://doi.org/10.1080/17518253.2018.1538430
13) Soltys, L., Olkhovyy, O., Tatarchuk, T., & Naushad, M. (2021). Green synthesis of metal and metal oxide nanoparticles: Principles of green chemistry and raw materials. *Magnetochemistry*, *7*(11), 145. https://doi.org/10.3390/magnetochemistry7110145.
14) MubarakAli, D., Thajuddin, N., Jeganathan, K., & Gunasekaran, M. (2011). Plant extract mediated synthesis of silver and gold nanoparticles and its antibacterial activity against clinically isolated pathogens. *Colloids and Surfaces B Biointerfaces*, *85*(2), 360–365. https://doi.org/10.1016/j.colsurfb.2011.03.009.
15) Ronavari, A., Igaz, N., Adamecz, D. I., Szerencsés, B., Molnar, C., Kónya, Z., Pfeiffer, I., & Kiricsi, M. (2021). Green Silver and Gold nanoparticles: biological synthesis approaches and potentials for biomedical applications. *Molecules*, *26*(4), 844. https://doi.org/10.3390/molecules26040844 .
16) Suresh, K. C., & Balamurugan, A. (2020). Evaluation of structural, optical, and morphological properties of nickel oxide nanoparticles for multi-functional applications. *Inorganic and Nano-Metal Chemistry*, *51*(2), 296–301. https://doi.org/10.1080/24701556.2020.1770793
17) Suresh, K. C., Surendhiran, S., Kumar, P. M., Kumar, E. R., Khadar, Y. a. S., & Balamurugan, A. (2020). Green synthesis of SnO_2 nanoparticles using Delonixelata leaf extract: Evaluation of its structural, optical, morphological and photocatalytic properties. *SN Applied Sciences*, *2*(10). https://doi.org/10.1007/s42452-020-03534-z
18) Suresh, D., Nethravathi, P., Udayabhanu, N., Rajanaika, H., Nagabhushana, H., & Sharma, S. (2015). Green synthesis of multifunctional zinc oxide (ZnO) nanoparticles using Cassia fistula plant extract and their photodegradative, antioxidant and antibacterial activities. *Materials science in semiconductor Processing,31,* 446-454. https://doi.org/10.1016/j.mssp.2014.12.023
19) Surendhiran, S., Gowthambabu, V., Balamurugan, A., Sudha, M., Kumar, V. S., & Suresh, K.C (2021). Rapid green synthesis of CuO nanoparticles and evaluation of its photocatalytic and electrochemical corrosion inhibition performance. *Materials Today Proceedings*, *47*, 1011–1016. https://doi.org/10.1016/j.matpr.2021.05.515.
20) Abdalameer, N. K., Khalaph, K. A., & Ali, E. M. (2021). Ag/AgO nanoparticles: Green synthesis and investigation of their bacterial inhibition effects. *Materials Today Proceedings*, *45*, 5788–5792. https://doi.org/10.1016/j.matpr.2021.03.166.
21) Kunoh, T., Takeda, M., Matsumoto, S., Suzuki, I., Takano, M., Kunoh, H., & Takada, J. (2017). Green Synthesis of Gold Nanoparticles Coupled with Nucleic Acid Oxidation. *ACS Sustainable Chemistry & Engineering*, *6*(1), 364–373. https://doi.org/10.1021/acssuschemeng.7b02610.
22) Wu, X. (2021). Applications of titanium dioxide materials. In *Intech Open eBooks*. https://doi.org/10.5772/intechopen.99255
23) Bekele, E. T., Gonfa, B. A., & Sabir, F. K. (2021). Use of different natural products to control growth of titanium oxide nanoparticles in green solvent emulsion, characterization, and their photocatalytic application. *Bioinorganic Chemistry and Applications*,1-17, https://doi.org/10.1155/2021/6626313
24) Waghmode, M. S., Gunjal, A. B., Mulla, J. A., Patil, N. N., & Nawani, N. N. (2019). Studies on the titanium dioxide nanoparticles: biosynthesis, applications and remediation. *SN Applied Sciences*, *1*(4). https://doi.org/10.1007/s42452-019-0337-3.
25) Haider, A. J., Anbari, R. H. A., Kadhim, G. R., & Salame, C. T. (2017). Exploring potential Environmental applications of TiO_2 Nanoparticles. *Energy Procedia*, *119*, 332–345. https://doi.org/10.1016/j.egypro.2017.07.117.
26) Kavitha, V., Mayandi, J., Mahalingam, P., & Sethupathi, N. (2019). Structural, optical and electrical studies on zinc doped barium strontium titanate as photo-anode for DSSC device. *Materials Today Proceedings*, *35*, 48–52. https://doi.org/10.1016/j.matpr.2019.05.437.

27) Ansari, A., Siddiqui, V. U., Rehman, W. U., Akram, M. K., Siddiqi, W. A., Alosaimi, A. M., Hussein, M. A., &Rafatullah, M. (2022). Green Synthesis of TiO_2 Nanoparticles Using Acorus calamus Leaf Extract and Evaluating Its Photocatalytic and In Vitro Antimicrobial Activity. *Catalysts*, *12*(2), 181. https://doi.org/10.3390/catal12020181.
28) Ansari, A., Siddiqui, V. U., Rehman, W. U., Akram, M. K., Siddiqi, W. A., Alosaimi, A. M., Hussein, M. A., & Rafatullah, M. (2022b). Green Synthesis of TiO_2 Nanoparticles Using Acorus calamus Leaf Extract and Evaluating Its Photocatalytic and In Vitro Antimicrobial Activity. *Catalysts*, *12*(2), 181. https://doi.org/10.3390/catal12020181.
29) Irshad, M. A., Nawaz, R., Rehman, M. Z. U., Imran, M., Ahmad, J., Ahmad, S., Inam, A., Razzaq, A., Rizwan, M., & Ali, S. (2020). Synthesis and characterization of titanium dioxide nanoparticles by chemical and green methods and their antifungal activities against wheat rust. *Chemosphere*, *258*, 127352. https://doi.org/10.1016/j.chemosphere.2020.127352.
30) Rusu, A., Predoană, L., Preda, S., Culiţă, D. C., & Zaharescu, M. (2024). FT-IR spectroscopy study of the TiO_2 based powders prepared by the sol-gel method. *Revue Roumaine De Chimie*, *69*(10–12), 629–634. https://doi.org/10.33224/rrch.2024.69.10-12.13.
31) Singh, P. K., Mukherjee, S., Ghosh, C. K., & Maitra, S. (2017). Spectroscopic Investigation on Sol Gel Derived TiO_2 Nanoparticles. *Journal of Advances in Nanomaterials*, *2*(3). https://doi.org/10.22606/jan.2017.23004.
32) Pugachevsky, M. A. (2012). Effect of annealing on photoluminescent properties of titanium dioxide nanoparticles. *Journal of Applied Spectroscopy*, *79*(5), 834–837. https://doi.org/10.1007/s10812-012-9680-5.
33) Al-Taweel, S. S., Saud, H. R., Kadhum, A. a. H., & Takriff, M. S. (2019). The influence of titanium dioxide nanofiller ratio on morphology and surface properties of TiO_2/chitosan nanocomposite. *Results in Physics*, *13*, 102296. https://doi.org/10.1016/j.rinp.2019.102296.
34) González, S., & Jaramillo-Fierro, X. (2025). Density Functional Theory Study of methylene blue demethylation as a key step in degradation mediated by reactive oxygen species. *International Journal of Molecular Sciences*, *26*(4), 1756. https://doi.org/10.3390/ijms26041756.
35) Kuila, S. K., Sarkar, R., Kumbhakar, P., Kumbhakar, P., Tiwary, C. S., & Kundu, T. K. (2020). Photocatalytic dye degradation under sunlight irradiation using cerium ion adsorbed two-dimensional graphitic carbon nitride. *Journal of Environmental Chemical Engineering*, *8*(4), 103942. https://doi.org/10.1016/j.jece.2020.103942.
36) Aravind, M., Amalanathan, M., & Mary, M. S. M. (2021). Synthesis of TiO_2 nanoparticles by chemical and green synthesis methods and their multifaceted properties. *SN Applied Sciences*, *3*(4). https://doi.org/10.1007/s42452-021-04281-5.
37) BinSabt, M., Sagar, V., Singh, J., Rawat, M., & Shaban, M. (2022). Green synthesis of CS-TIO2 NPS for efficient photocatalytic degradation of methylene blue dye. *Polymers*, *14*(13), 2677. https://doi.org/10.3390/polym14132677

****